RSC Advances

PAPER

View Article Online
View Journal | View Issue

Cite this: *RSC Adv.*, 2025, **15**, 11549

Megastigmanes isolated from *Boehmeria nivea* leaves and their immunomodulatory effect on IL-1β and IL-10 production in RAW264.7 macrophages†

Thi Thu Thao Nguyen, [ab] Vy Anh Tran,[c] Thi Hien Tran,[d] Viet Duc Ho,[e] Thi Ha Do,[f] Quoc Ky Truong,[g] Minh Quan Pham[hi] and Thi Hong Van Le *[a]

With the aim of isolating immunomodulatory compounds from the *n*-butanol extract of *Boehmeria nivea* leaves, nine megastigmane compounds were identified. Among these, the structure of the new compound **1**, namely, "boehmegaside A", was established using NMR and HR-ESI-MS, and its absolute configurations were established through ECD calculations and DP4+ analysis using DFT-NMR chemical shift calculations. Furthermore, eight of these compounds were discovered for the first time in the *Boehmeria* genus, marking this the first report on megastigmane compounds isolated from this genus. Regarding their immunomodulatory activity, the isolated megastigmane compounds **3**, **2**, and **6** exhibited pro-inflammatory cytokine IL-1β secretion inhibitory activity. Compounds **3** and **6** significantly increased anti-inflammatory cytokine IL-10 secretion in LPS-activated RAW264.7 cells. Furthermore, the study on the mechanism of the immunomodulatory and other biological activities of megastigmane compounds through molecular docking simulations revealed that the planar structures of **3**, **2**, and **6** were critical in their ability to directly suppress TLR4 signalling. Instead, they attached to a nearby smooth area in TLR4. This interference likely disrupted the ability of TLR4 and MD-2 to form their primary contact interface and recognize LPS. These findings highlight the significant role of TLR4 in inflammation and immunity, indicating that these megastigmane compounds may be beneficial in treating various inflammatory disorders associated with immunological issues.

Received 10th September 2024
Accepted 24th March 2025

DOI: 10.1039/d4ra06545j

rsc.li/rsc-advances

Introduction

Various infectious diseases, inflammatory diseases, asthma, autoimmune diseases, tumor formation, cancer development, and disorders are related to the immune system. The immune system is a remarkably complex defense system that protects against foreign pathogens and infectious agents. It can generate varieties of cells and chemical mediators to recognize and eliminate limitless varieties of foreign and undesirable agents. Modulation of the immune system denotes any change in the immune response, which could involve the induction, expression, amplification, or inhibition of any part or phase of the immune response. Thus, an immunomodulator is a substance that affects the immune system.[1] Immunomodulation using medicinal plants can provide an alternative to conventional chemotherapy for various diseases, mainly when a host defense mechanism must be acquired under a state of impaired immune responsiveness.[2] In Vietnam, research on immunomodulatory activities is still limited. Furthermore, compared with the vast medicinal resources, only few plants have been screened for immunomodulatory activities. Although there are several medicinal plants and marine products that possess immunomodulatory activity, inadequate evidence does not allow their use in clinical practice. This suggests that immunomodulatory agents will gain more importance in future research on herbal medicine.

Several methods for the pharmacological screening of medicinal plants with immunomodulatory activity have been used based on immunological factors. Among them,

[a]*Faculty of Pharmacy, University of Medicine and Pharmacy at Ho Chi Minh City, Vietnam. E-mail: levan@ump.edu.vn*
[b]*University of Health Sciences, Vietnam National University, Ho Chi Minh City, Vietnam*
[c]*Department of Material Science, Institute of Applied Technology and Sustainable Development, Nguyen Tat Thanh University, Ho Chi Minh City, Vietnam*
[d]*Department of Microbiology, Immunology and Glycobiology, Institute of Laboratory Medicine, Lund University, Box 117, Lund, SE-221 00, Sweden*
[e]*Faculty of Pharmacy, Hue University of Medicine and Pharmacy, Hue University, 06 Ngo Quyen, Hue City, Vietnam*
[f]*Department of Medical Plant Chemistry, National Institute of Medical Materials (NIMM), Hanoi, 11022, Vietnam*
[g]*Faculty of Pharmacy, Pham Ngoc Thach University of Medicine, Ho Chi Minh City, Vietnam*
[h]*Institute of Natural Products Chemistry, Vietnam Academy of Science and Technology, Hanoi, Vietnam*
[i]*Graduate University of Science and Technology, Vietnam Academy of Science and Technology, Hanoi, Vietnam*

† Electronic supplementary information (ESI) available. See DOI: https://doi.org/10.1039/d4ra06545j

interleukin-1β (IL-1β) and interleukin-10 (IL-10) cytokines are potential targets for immune therapy. IL-1β is a pro-inflammatory cytokine involved in immune responses and inflammation, and it can contribute to carcinogenesis, tumor growth, and invasion.[3] IL-10, in contrast, is an important cytokine with anti-inflammatory properties and regulates the functions of various immune cells.[4] The role of IL-10 in cancer is complex, with both tumor-promoting and tumor-repressing effects. On the one hand, IL-10 can inhibit the activation of cytotoxic T cells by reducing the expression of major histocompatibility complexes on cancer cells and antigen-presenting cells, thereby impeding the recognition and targeting of cancer cells by antigen-specific T cells. On the other hand, studies have shown that high doses of IL-10 can enhance the proliferation and cytotoxic activity of CD8+ T cells.[5]

Boehmeria nivea (L.) Gaudich, Urticaceae is a versatile plant that has been utilized for many purposes, including food, animal feed, medicinal applications, and fiber production. The root of this plant is used in traditional Chinese herbal medicine to treat the common cold, edema, fever, fetal irritability, urinary tract infections, nephritis, and abortion risk, and it possesses various pharmacological properties. Its leaves have been reported to have antibiotic and anti-inflammatory effects.[6] Numerous studies have shown that the extract of *Boehmeria nivea* leaves (BNL) exerts many biological activities, such as anti-proliferative, antitumor, anti-inflammatory, antibacterial, anti-oxidant, glucose-lowering, and anti-hepatitis B virus effects.[7] Nevertheless, studies on the chemical components have shown that these leaves contain several common ingredients, including flavonoids, simple phenols, sterols, terpenoids, coumarins, anthraquinones, reducing sugars, fatty acids, and polysaccharides.[8] In an ongoing investigation into the immune-inducing activity of some Vietnamese medicinal plants, it was found that a 70% ethanol BNL extract had immunomodulatory activity against IL-1β and IL-10 cytokines production in RAW 264.7 murine macrophages; therefore, this plant was selected for further study. Consequently, this study aimed to investigate the immunomodulatory effects of BNL extracts in a RAW 264.7 macrophage cell line, and then isolate and elucidate the chemical components from the active extract of *B. nivea* leaves. In our recent publication, we identified 8 compounds belonging to neolignan, phenolic and sugar derivatives from *B. nivea*, namely glochidioboside, protocatechuic acid, ethyl β-fructopyranoside, glycerol, eugenyl *O*-β-apiofuranosyl-(1″ → 6′)-*O*-β-glucopyranoside, ethyl α-D-glucopyranoside, hydroxytyrosol 4-β-D-glucoside, and cimidahurinine, in the active extract (*n*-butanol).[9]

In this article, we report on the immunomodulatory effects of BNL extracts in a RAW 264.7 macrophage cell line, as well as the isolation and structural identification of 9 compounds belonging to megastigmane from bioassay-guided isolation processing of an *n*-butanol extract. We also investigated the immunomodulatory activity of certain compounds from the leaves of *B. nivea* on the secretion of the pro-inflammatory cytokine IL-1β and on anti-inflammatory cytokines IL-10 production in RAW 264.7 macrophages.

Results and discussion

Screening the immunomodulatory activity of the fractionated extracts

The effects of the extracts (*n*-hexane, EtOAc, *n*-butanol) at 20 μg mL^{-1} on the secretion of the pro-inflammatory cytokine IL-1β and on anti-inflammatory cytokines IL-10 production in RAW 264.7 macrophages were quantified by ELISA analysis, and the results are presented in Fig. 1 and 2.

The results on IL-1β showed that with the action of LPS, the RAW 264.7 cells increased IL-1β secretion (at 24 h). When treating the RAW264.7 cells with the BNL extracts, three extracts enormously reduced IL-1β to levels ranging from 46.61 to 63.67 pg mL^{-1}, compared to the LPS-positive control group with a concentration of 434.82 pg mL^{-1} ($p < 0.0001$).

Furthermore, upon testing against IL-10 cytokines, all the extracts showed enormously increased IL-10 production, with levels ranging from 267.07 to 292.98 pg mL^{-1} compared to the LPS-positive control group, with a concentration of 109.79 pg mL^{-1} ($p < 0.0001$ and $p < 0.001$). Among them, the polar extract (*n*-BuOH) showed the most potent immunomodulatory activity through inhibiting IL-1β and stimulating IL-10 production ($p < 0.0001$ and $p < 0.001$). Consequently, the *n*-BuOH extract was chosen to investigate the chemical composition.

Structure elucidation of the megastigmane compounds

To the best of our knowledge, this study is the first report about the megastigmane group in *Boehmeria* genus, specifically, a new megastigmane compound in nature, and 8 new megastigmane compounds in the genus *Boehmeria*. The 1D and 2D-NMR data of new megastigmane compound are presented in Table 2, and ^{1}H-NMR and ^{13}C-NMR spectrum data of the other megastigmane compounds are presented in Tables 3 and 4.

Compound **1** was a colorless gum. The molecular formula was determined to be $C_{19}H_{30}O_7$ from the HR-ESI-MS (positive mode) *m*/*z*: 393.20361 $[M + Na]^+$ (calcd. for $C_{19}H_{30}O_7Na$, 393.20392). The ^{1}H and ^{13}C-NMR spectra showed a typical pattern of megastigmane glycoside. Spectroscopic data showed that **1** was a megastigmane glycoside with the following data: the ^{1}H-NMR spectrum of **1** showed an olefin proton C=CH at δ_H 5.91 (1H; d; $J = 1.5$; H-4) and 2 protons of trans olefin (CH=CH) at δ_H 5.58 (1H; dd; $J = 15.4$, 9.0; H-7) and 5.66 (1H, dd, $J = 15.4$, 7.0; H-8); 1 methylene group [δ_H 2.35 (1H; d; $J = 16.8$ Hz, H-2a)/ 2.06 (1H; d; $J = 16.8$ Hz; H-2b)]; 1 oxymethine group [4.30 (1H; m; H-9)], and 4 methyl groups. Furthermore, the ^{1}H-NMR spectrum displayed the signal of an anomer proton at δ_H 4.34 (1H, d, $J = 7.58$ Hz, H-1′), with 2 hydroxy methylene protons and hydroxy methine proton signals located in the range of 3.21–3.82 ppm, suggesting the presence of a sugar unit in a β configuration. The ^{13}C-NMR data (Table 2), assigned with the aid of the HSQC and HMBC spectra, displayed 19 carbon resonances, including 13 carbon resonances of the megastigmane structure [3 quaternary carbons with a carbonyl group at δ_C 199.7 (C-3); 2 methine olefin groups at δ_C 128.3 (C-7) and 136.2 (C-8), another olefin carbon of CH=C at 125.8 (C-4); an oxymethine at δ_C 77.6 (C-9); a methylene at δ_C 47.2 (C-2); 4 methyl groups at δ_C 21.4 (C-

No	IL-1β Concentration (pg/mL)				
	n-Hexane	EtOAc	*n*-BuOH	DMSO	LPS
1	70.74	49.27	45.34	164.74	**368.77**
2	55.16	55.92	58.36	149.81	**447.98**
3	57.18	49.51	49.84	126.19	**476.46**
4	63.78	55.07	40.26	129.15	**385.65**
5	71.49	48.34	39.26	115.55	**495.26**
Average	**63.67**	**51.62**	**46.61**	**137.09**	**434.82**
SE	**3.36**	**1.60**	**3.50**	**8.87**	**24.84**

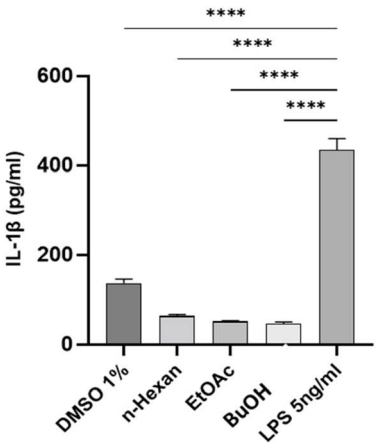

Fig. 1 Effects of extracts from BNL on the pro-inflammatory cytokine IL-1 β. Note: (****$p < 0.0001$) when compared with the LPS-positive control group ($n = 5$).

No	IL-10 Concentration (pg/mL)				
	n-Hexane	EtOAc	*n*-BuOH	DMSO	LPS
1	236.35	241.97	189.56	117.07	**126.96**
2	334.65	353.25	315.64	145.56	**88.58**
3	253.52	372.83	285.05	135.82	**122.75**
4	330.89	203.85	278.01	131.56	**100.88**
5	260.95	220.26	251.28	122.39	**102.28**
Average	**288.85**	**292.98**	**267.07**	**132.50**	**109.79**
SE	**20.61**	**35.20**	**21.22**	**5.01**	**7.20**

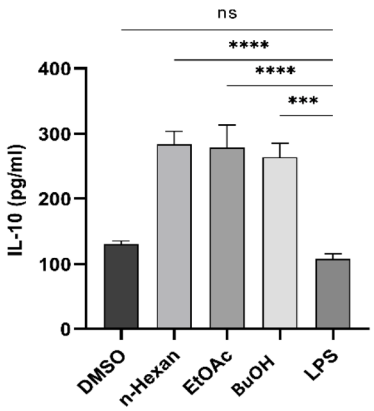

Fig. 2 Effects of extracts from BNL on the anti-inflammatory cytokine IL-10. Note: (****$p < 0.0001$, ***$p < 0.001$, ns > 0.05) when compared with the LPS-positive control group ($n = 5$).

10), 23.7 (C-13), 27.4 (C-11), 27.8 (C-12)] and 6 carbons of a sugar unit glucopyranose [δ_C 101.7(C-1′)]. The sugar unit was confirmed as being linked at C-9 by HMBC correlation of the anomeric proton (H-1) with C-9 (δ_C 77.6).

On the other hand, the monosaccharide composition, sugar moiety linkage, and the attachment site of the sugar moiety to the aglycone were determined by NMR spectroscopic analyses combined with the acid hydrolysis of **1** followed by reduction, per-acetylated derivatization, and GC-MS analysis. The acid hydrolysis revealed the presence of the D-glucose moiety in **1**. This was deduced to be the hexose moiety in the D-glucopyranose form based on the corresponding resonances in the ^{1}H and ^{13}C-NMR spectra (Tables 2 and 3) and the correlations observed in the ^{1}H–^{1}H COSY and HMBC spectra (Fig. 3A). Furthermore, the coupling constant of 7.58 Hz between H-1′ and H-2′ indicated the β-configuration at the respective anomeric position of the D-glucopyranose moiety (Fig. 3A). To clarify the stereochemistry of the aglycone moiety of **1**, DFT-NMR chemical shift calculations coupled with the DP4+ probability method were applied for four diastereomers: (6*R*,9*R*)-**1a**, (6*R*,9*S*)-**1b**, (6*S*,9*R*)-**1c**, and (6*S*,9*S*)-**1d** (see the ESI†). Briefly, the conformational searches using the molecular mechanics set yielded 6, 4, 6, and 6 main conformers, with Boltzmann distributions > 1%, for **1a–1d**, respectively. The main conformers were further DFT optimized, and the harmonic vibrational frequencies were calculated at the B3LYP/6-31G(d) level in the gas phase. Finally, the ^{1}H and ^{13}C chemical shifts of the optimized conformers were calculated using Gaussian 09 with

Table 1 DP4+ analyses and probability scores of 4 diastereomers of compound **1**

Diastereomers	6*R*,9*R* (**1a**)	6*R*,9*S* (**1b**)	6*S*,9*R* (**1c**)	6*S*,9*S* (**1d**)
mPW1PW91/6-31G+(d,p)/PCM				
DP4+ (H data)	0.08%	0.01%	0.07%	0.00%
DP4+ (C data)	34.22%	0.00%	65.78%	0.00%
DP4+ (all data)	37.37%	0.00%	62.63%	0.00%
mPW1PW91/6-311G(d,p)/PCM				
DP4+ (H data)	0.02%	0.45%	99.53%	0.00%
DP4+ (C data)	0.03%	0.03%	99.93%	0.00%
DP4+ (all data)	0.00%	0.00%	100%	0.00%

Table 2 1D and 2D NMR spectral data of compound **1**

Position	Type	δ_C[a] (CD_3OD)	δ_C[b] ($CDCl_3$)	δ_H[b] (m, *J* Hz, nH) ($CDCl_3$)	HMBC[b] ($CDCl_3$)	COSY[b] ($CDCl_3$)
1	C	37.2	36.2	—	—	—
2	CH_2	48.4	47.2	2.35 (d, 16.8 Hz, 1H)	1, 3, 12	—
				2.06 (d, 16.8 Hz, 1H)	—	—
3	C	202.1	199.7	—	—	—
4	CH	126.1	125.8	5.91 (d, 1.5 Hz, 1H)	2, 6, 13	—
5	C	166.0	162.5	—	—	—
6	CH	56.8	55.3	2.53 (d, 8.8 Hz, 1H)	2, 4, 5, 7, 8, 11, 13	—
7	CH	128.9	128.3	5.58 (dd, 15.4, 8.8 Hz, 1H)	8, 6, 1	8, 6
8	CH	138.4	136.2	5.66 (dd, 15.4, 7.0 Hz, 1H)	7, 6, 10	7, 9
9	CH	78.1	77.6	4.30 (m, 1H)	8, 7, 10	10
10	CH_3	21.1	21.4	1.30 (d, 6.4 Hz, 3H)	8, 9	—
11	CH_3	27.4	27.4	0.96 (d, 7.0 Hz, 3H)	1, 2, 6	—
12	CH_3	28.0	27.8	1.03 (s, 3H)	1, 2, 6	—
13	CH_3	23.9	23.7	1.90 (m, 3H)	5, 4	—
1′	CH	102.5	101.7	4.34 (d, 7.8 Hz, 1H)	9	2′
2′	CH	75.3	73.5	3.35 (t, 8.4 Hz, 1H)	1′, 3′	—
3′	CH	78.0	76.3	3.48 (m, 1H)	4′	—
4′	CH	71.5	69.3	3.59 (t, 9.6 Hz, 1H)	3′, 6′	—
5′	CH	77.0	75.7	3.21 (m,1H)	—	4′
6′	CH_2	62.7	61.3	3.82 (d, 12.0 Hz, 1H)	—	—
				3.73 (d, 12.0 Hz, 1H)	—	—

[a] ^{13}C-NMR: 150 MHz. [b] ^{13}C-NMR: 150 MHz, ^{1}H-NMR: 600 MHz.

Table 3 ^{13}C NMR spectral data of the nine megastigmane compounds[a]

Position	**1**[b]	**2**[c]	**3**[c]	**4**[c]	**5**[d]	**6**[c]	**7**[d]	**8**[e]	**9**[e]
1	36.2, C	42.4, C	39.9, C	35.9, C	36.7, C	35.3, C	45.3, C	32.9, C	34.0, C
2	47.2, CH_2	50.7, CH_2	54.4, CH_2	45.7, CH_2	48.7, CH_2	44.9, CH_2	50.1, CH_2	47.7, CH_2	54.6, CH_2
3	199.7, C=O	201.2, C=O	201.9, C=O	73.0, CH	65.4, CH	72.3, CH	77.6, CH	73.1, CH	209.3, C=O
4	125.8, CH	127.2, CH	127.1, CH	38.5, CH_2	42.4, CH_2	37.6, CH_2	49.5, CH_2	46.7, CH_2	55.9, CH_2
5	162.5, C	167.2, C	159.0, C	67.7, C	68.9, C	67.4, C	83.0, C	87.7, C	89.0, C
6	55.3, CH	80.0, C	145.0, C	71.4, C	71.9, C	69.6, C	93.5, C	153.9, C	150.7, C
7	128.3, CH	131.6, CH	135.2, CH	125.8, CH	130.4, CH	142.1, CH	127.4, CH	117.3, CH	120.5, CH
8	136.2, CH	135.3, CH	71.3, CH	139.1, CH	136.8, CH	132.7, CH	135.1, CH	86.9, CH	86.8, CH
9	77.6, CH	77.3, CH	79.5, CH	68.4, CH	75.5, CH	197.4, C	78.9, CH	69.6, CH	75.6, CH
10	21.4, CH_3	21.2, CH_3	15.4, CH_3	23.8, CH_3	23.2, CH_3	28.3, CH_3	22.2, CH_3	17.1, CH_3	13.7, CH_3
11	27.4, CH_3	23.4, CH_3	29.8, CH_3	25.2, CH_3	30.9, CH_3	24.9, CH_3	26.7, CH_3	26.0, CH_3	26.7, CH_3
12	27.8, CH_3	24.7, CH_3	29.7, CH_3	29.8, CH_3	25.8, CH_3	29.4, CH_3	33.6, CH_3	29.9, CH_3	29.4, CH_3
13	23.7, CH_3	19.6, CH_3	22.8, CH_3	20.3, CH_3	21.5, CH_3	19.8, CH_3	32.3, CH_3	26.1, CH_3	26.9, CH_3
1′-*O*-Glc	101.7, CH	102.8, CH	103.0, CH	102.9, CH	102.1, CH	101.5, CH	103.6, CH	101.4, CH	100.7, CH
2′	73.5, CH	75.3, CH	75.0, CH	75.2, CH	75.9, CH	75.6, CH	76.2, CH	73.8, CH	73.8, CH
3′	76.3, CH	78.1, CH	77.9, CH	78.2, CH	78.9, CH	76.5, CH	78.9, CH	76.7, CH	76.6, CH
4′	69.3, CH	71.7, CH	71.6, CH	71.6, CH	72.6, CH	69.5, CH	72.2, CH	70.4, CH	70.5, CH
5′	75.7, CH	78.0, CH	78.0, CH	77.8, CH	78.9, CH	73.4, CH	78.8, CH	76.6, CH	76.7, CH
6′	61.3, CH_2	62.9, CH_2	62.7, CH_2	62.7, CH_2	63.7, CH_2	61.5, CH_2	63.5, CH_2	61.5, CH_2	61.6, CH_2

[a] Abbreviation Glc = glucopyranoside. [b] $CDCl_3$, ^{13}C-NMR: 150 MHz, ^{1}H-NMR: 600 MHz. [c] CD_3OD, ^{13}C-NMR: 150 MHz, ^{1}H-NMR: 600 MHz. [d] CD_3OD, ^{13}C-NMR: 200 MHz, ^{1}H-NMR: 800 MHz. [e] CD_3OD, ^{13}C-NMR: 125 MHz, ^{1}H-NMR: 500 MHz.

GIAO/mPW1PW91/6-31+G(d,p)/PCM/chloroform and GIAO/mPW1PW91/6-311G(d,p)/PCM/chloroform. Shielding tensors were used for the DP4+ probability calculations. As a result, DP4+ analysis showed that the most probable structure was (6*S*,9*R*)-**1c** (Table 1). Furthermore, the predicted ECD curves were carefully evaluated for the four diastereomers, whereupon it was found that the experimental ECD spectrum of **1** was in good agreement with the predicted ECD curves of (6*S*,9*R*)-**1c**; and (6*S*,9*S*)-**1d** (Fig. 3B). Combining the ECD and DP4+ analyses, **1** was elucidated as (6*S*,9*R*)-3-oxo-α-ionol-β-D-glucopyranoside and was named boehmegaside A.

In addition, the 9*R* configuration was strengthened by the agreement of the chemical shift of C-9 (δ_C 78.1) with that of (9*R*)-3-oxo-ionol (δ_C 77.0), but being quite different from that of (9*S*)-3-oxo-ionol (δ_C 74.7) in CD_3OD.[10,11] Meanwhile, the 6*S* configuration was confirmed by the fact that the ECD spectrum of **1** [$\Delta\varepsilon$: −28.90 (245 nm), + 1.15 (319 nm)] showed almost the same tendency to the ECD data of (6*S*,9*R*)-3-oxo-α-ionol-9-*O*-β-D-

Table 4 ^{1}H-NMR spectral data $^{\delta}$H (m, *J* Hz, nH) of the nine megastigmane compounds[a]

Position	**1** [b]	**2** [c]	**3** [c]	**4** [c]	**5** [d]	**6** [d]	**7** [d]	**8** [e]	**9** [e]
1	—	—	—	—	—	—	—	—	—
2	2.35 (d, 16.8, 1H)	2.51 (d, 17.0, 1H)	2.39 (d, 2.4, 2H)	1.35 (dd, 13.1, 10.4,1H)	1.22 (m, 1H)	1.73 (m, 1H)	1.76 (ddd, 11.6, 6.0, 2.4, 1H)	1.27 (m, 1H)	2.21 (dd, 13.5, 2.0, 1H)
	2.06 (d, 16.8, 1H)	2.15 (d, 17.0, 1H)	—	1.72 (m, 1H)	1.54 (ddd, 12.8, 3.4, 1.8, 1H)	1.35 (m, 1H)	1.58 (d, 11.6, 1H)	1.96 (ddd, 12.7, 4.2, 2.0, 1H)	2.42 (d, 13.5, 1H)
3	—	—	—	3.89 (dddd, 10.4, 8.5, 5.0, 3.5, 1H)	3.74 (m, 1H)	3.88 (m, 1H)	4.33 (t, 6.0, 1H)	4.08 (tt, 11.8, 4.2, 1H)	—
4	5.91 (d, 1.5, 1H)	5.87 (t, 1.26, 1H)	5.98 (1H, s)	1.75 (dd, 14.4, 8.5, 1H)	1.61 (dd, 14.2, 9.0, 1H)	2.45 (d, 14.1, 1H)	1.94 (ddd, 11.6, 6.0, 2.4, 1H)	1.48 (m, 1H)	2.56 (dd, 12.9, 2.0, 1H)
	—	—	—	2.39 (ddd, 14.4, 5.0, 1.7, 1H)	2.27 (ddd, 14.2, 5.0, 1.8, 1H)	1.73 (m, 1H)	1.64 (d, 12, 1H)	2.36 (ddd, 11.5, 4.2, 2.0. 1H)	2.84 (dt, 12.9, 1.0, 1H)
5	—	—	—	—	—	—	—	—	—
6	2.53 (d, 8.8, 1H)	—	—	—	—	—	—	—	—
7	5.58 (dd, 15.4, 8.8, 1H)	5.86 (m, 1H)	6.12 (d, 9.2, 1H)	5.91 (dd, 15.4, 1.3, 1H)	6.05 (dd, 15.5, 1.0, 1H)	7.0 (dd, 15.6, 3.8, 1H)	5.79 (d, 16, 1H)	5.39 (d, 1.0, 1H)	5.79 (d, 1.2, 1H)
8	5.66 (dd, 15.4, 7.0, 1H)	5.85 (m, 1H)	4.95 (1H, dd, 9.2, 4.0)	5.67 (dd, 15.4, 6.0, 1H)	5.57 (dd, 15.5, 7.5, 1H)	6.26 (dd, 15.6, 4.6, 1H)	5.74 (dd, 16, 6.4, 1H)	4.59 (dd, 5.3, 1.0, 1H)	4.86 (dd, 4.4, 1.2, 1H)
9	4.3 (m, 1H)	4.42 (pd, 6.6, 4.4, 1H)	3.99 (1H, qd, 6.4, 4.0)	4.28 (dquin, 6.0, 1.3, 1H)	4.52 (m, 1H)	—	4.39 (p, 6.4, 1H)	3.61 (m, 1H)	3.94 (qd, 6.4, 4.4, 1H)
10	1.30 (d, 6.4, 3H)	1.29 (d, 6.6, 3H)	1.26 (3H, d, 6.4)	1.22 (d, 6.4, 3H)	1.27 (d, 6.4, 3H)	2.28 (d, 4.6, 3H)	1.29 (d, 6.4, 3H)	1.09 (d, 6.4, 3H)	1.16 (d, 6.4, 3H)
11	0.96 (d, 7.0, 3H)	1.04 (s, 3H)	1.36 (s, 3H)	0.96 (s, 3H)	1.11 (s, 3H)	0.97 (d, 3.8, 3H)	1.39 (s, 3H)	1.13 (s, 3H)	1.11 (s, 3H)
12	1.03 (s, 3H)	1.03 (s, 3H)	1.40 (s, 3H)	1.14 (s, 3H)	0.93 (s, 3H)	1.17 (s, 3H)	0.84 (s, 3H)	1.20 (s, 3H)	1.32 (s, 3H)
13	1.90 (m, 3H)	1.92 (d, 1.4,3H)	2.16 (s, 3H)	1.19 (s, 3H)	1.24 (s, 3H)	1.19 (d, 4.4, 3H)	1.18 (s, 3H)	1.39 (d, 1.0, 3H)	1.38 (s, 3H)
1′-OGlc	4.34 (d, 7.8, 1H)	4.34 (d, 7.8, 1H)	4.40 (d, 7.8, 1H)	4.33 (d, 7.8, 1H)	4.27 (d, 7.8, 1H)	4.39 (d, 7.6, 1H)	4.35 (d, 7.8, 1H)	4.37 (d, 7.8, 1H)	4.33 (d, 7.7, 1H)
2′	3.35 (t, 8.4, 1H)	3.17 (dd, 9.2, 7.8, 1H)	3.22 (dd, 9.1, 7.8, 1H)	3.12 (dd, 9.0, 7.8, 1H)	3.18 (m, 1H)	3.31 (m, 1H)	3.17 (m, 1H)	3.10 (dd, 9.2, 7.8, 1H)	3.14 (dd, 9.3, 7.7, 1H)
3′	3.51 (m, 1H)	3.33 (m, 1H)	3.40 (m, 1H)	3.34 (t, 9.0, 1H)	3.25 (m, 1H)	3.52 (m, 1H)	3.32 (m, 1H)	3.25 (m, 1H)	3.33 (m, 1H)
4′	3.59 (t, 9.6, 1H)	3.26 (d, 9.8, 1H)	3.44 (m, 1H)	3.28 (m, 1H)	3.25 (m, 1H)	3.58 (m, 1H)	3.30 (m, 1H)	3.25 (m, 1H)	3.23 (m, 1H)

Table 4 (*Contd.*)

Position	1 [b]	2 [c]	3 [c]	4 [c]	5 [d]	6 [d]	7 [d]	8 [e]	9 [e]
5′	3.21 (m, 1H)	3.23 (m, 1H)	3.39 (t, 8.7 1H)	3.26 (m, 1H)	3.16 (m, 1H)	3.33 (m, 1H)	3.18 (m, 1H)	3.33 (m, 1H)	3.23 (m, 1H)
6′	3.82 (d, 12.0, 1H)	3.85 (dd, 11.8, 2.2, 1H)	3.88 (dd, 11.6, 2.0, 1H)	3.67 (dd, 12, 5.3, 1H)	3.63 (dd, 12.0, 6.2, 1H)	3.83 (s, 2H)	3.81 (dd, 11.9, 2.4, 1H)	3.65 (dd, 5.6, 2.2, 1H)	3.62 (dd, 11.1, 5.2, 1H)
	3.73 (d, 12.0, 1H)	3.62 (dd, 11.8, 5.5, 1H)	3.69 (dd, 11.7 5.0, 1H)	3.84 (dd, 12, 2.3, 1H)	3.85 (dd, 12.0, 2.4, 1H)		3.65 (dd, 11.9, 5.3, 1H)	3.84 (m, 1H)	3.84 (dd, 11.7, 1.71H)

[a] Abbreviation Glc = glucopyranoside. [b] $CDCl_3$, ^{13}C-NMR: 150 MHz, ^{1}H-NMR: 600 MHz. [c] CD_3OD, ^{13}C-NMR: 150 MHz, ^{1}H-NMR: 600 MHz. [d] CD_3OD, ^{13}C-NMR: 200 MHz, ^{1}H-NMR: 800 MHz. [e] CD_3OD, ^{13}C-NMR: 125 MHz, ^{1}H-NMR: 500 MHz.

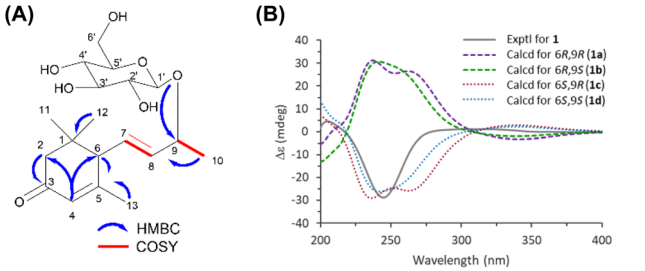

Fig. 3 HMBC, COSY interactions of 1 (A). Experimental and calculated ECD spectra of compound **1** in MeOH, σ 0.3 eV, and UV shift = +5 nm (B).

glucopyranosyl (1 → 2)-β-D-glucopyranoside [$\Delta\varepsilon$: −54.11 (243 nm), + 2.34 (310 nm)],[12] but opposite to that of the C-6*R* absolute configuration (the positive Cotton effects at 249 nm of two published isomers (6*R*,9*R*) and (6*R*,9*S*) 3-oxo-α-ionol-β-D-glucopyranoside).[10] Therefore, based on the above argument, the absolute configuration of compound **1** was completely suitable with the above computationally calculated results.

Compound **2** was obtained as a colorless gum, with the molecular formula of $C_{19}H_{30}O_8$ as deduced from the HR-ESI-MS peak at *m*/*z* 409.1823 $[M + Na]^+$ (calcd for $C_{19}H_{30}O_8Na$ 409.1838). The ^{1}H and ^{13}C-NMR spectra were almost identical to those of **1**, showing a typical pattern of megastigmane glycoside, with the only difference being in their chemical shifts observed at C-6 (due to the change from a tertiary carbon to quaternary carbon). The complete planar structure of **2** was determined by 2D NMR analysis (^{1}H–^{1}H COSY, HSQC, and HMBC), and was namely roseoside. The 6*S*,9*R* configuration of **2** was determined based on the chemical shifts of the carbon at positions C-7, C-8, and C-9 compared to the published spectroscopic data of the four diastereomers of roseoside in the same ref. 13 Based on the above results, **2** was identified as (6*S*,9*R*)-roseoside (Fig. 4).

Compound **3** was isolated as a colorless gum. It had the same molecular formula ($C_{19}H_{30}O_8$) as **2**, as deduced by the HR-ESI-

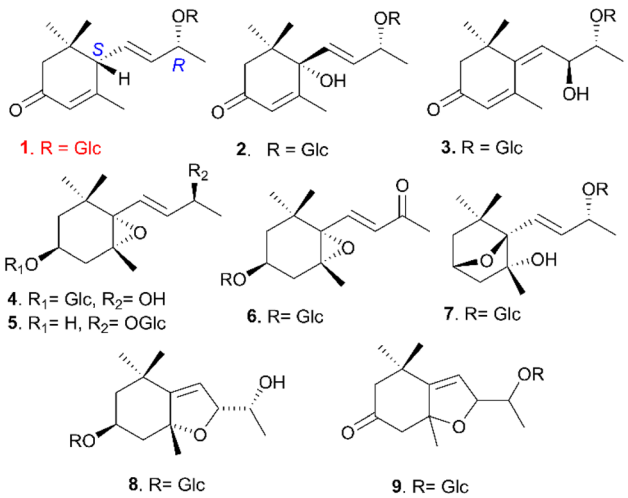

Fig. 4 Structures of megastigmane compounds isolated from *B. nivea* leaves.

MS peak at *m*/*z* 409.18714 $[M + Na]^+$(calcd. for $C_{19}H_{30}O_8Na$ 409.1838). The ^1H and ^{13}C-NMR spectra were almost identical to those of **2**, with the only differences being in their chemical shifts observed at C-6 and C-8 due to changes in the double bond and OH group positions. The complete planar structure of **3**, was determined as 8 hydroxymegastigmane-4,6-dien-3-on-9-*O*-β-D-glucopyranoside. The relative configuration of **3** was proposed from a NOESY experiment and by comparison of the observed and reported NMR data.[14] In the NOESY spectrum, the correlations between H-9 and H-1′ were tentatively assigned to an α-orientation. In addition, the NOESY spectrum also showed interactions between protons H-8 and H-12, H-8 and H-7, H-8 and H-9; consequently, H-8 was in the same direction as H-7, H-9 and H-12 (α orientation). Accordingly, the structure of **3** was proposed as 8*S*,9*R*-megastigman-3-one-4,6-diene-8,9-diol-9-*O*-β-D-glucopyranoside, also named as akequintoside D (Fig. 4).

Compound **4** was a colorless gum. Its identified molecular formula was $C_{19}H_{32}O_8$ based on the HR-ESI-MS peak at *m*/*z* 411.1966 $[M + Na]^+$ (calcd for $C_{19}H_{32}O_8Na$ 411.1989) in combination with the NMR data. The ^1H and ^{13}C-NMR spectra of **4** displayed typical signals for a megastigmane-type skeleton. The coupling constant (J = 7.8 Hz) of the anomeric proton signal was assigned as β-D-glucopyranose. The position of the sugar unit was confirmed by the HMBC correlation observed for the anomeric proton (H-1) with C-3 (δ_C 73.0). The complete planar structure of **4** was determined by 2D-NMR analysis (^1H–^1H COSY, HSQC, and HMBC). In addition, as with the current data, to meet the requirements for the molecular formula and unsaturation, compound **4**, needed to contain an epoxy ring, which was suggested to be formed between C-5 (δ_C 67.7) and C-6 (δ_C 71.4). Although the stereochemistry at C-5, C-6, and C-9 could not be established from the available data, the similarity between all the NMR data suggested that **4** may have the same stereoisomeric structure as alangionoside E[15] (Fig. 4).

Compound **5** was also a colorless gum. It had the same molecular formula as **4** $C_{19}H_{32}O_8$ (M = 388.2019, with unsaturation Δ = 4) according to the Q-Tof-MS spectrum *m*/*z* 411.2014 $[M + Na]^+$. Its NMR spectrum was quite similar to that of compound **4**, with the only difference being that part of the sugar was linked to the main frame at C-9. With these spectrum data, **5** was identified as 3-hydroxy-5,6-epoxy-β-ionol-9-*O*-β-D-glucopyranoside. This planar structure was similar to the structure of the two announced compounds staphylionoside H and phlomuroside (two diastereomers only different in the C-9 configuration). When comparing the spectroscopic data of **5** with the spectroscopic data of these two substances, it was found that the chemical shift and peak splitting of **5** were highly similar to those of compound staphylionoside H (9*S* configuration).[16] In addition, the identification with the 9*S* configuration was strengthened by the agreement of the chemical shift of C-9 with that of (9*S*)-3-oxo-ionol (δ_C 74.7), while being quite different from that of (9*R*)-3-oxo-ionol (δ_C 77).[10,11] From the above arguments, it could be concluded that **5** was staphylionoside H (Fig. 4).

Compound **6** was also a colorless gum. It had the same molecular formula as $C_{19}H_{30}O_8$ and was deduced by the HR-ESI-MS peak at *m*/*z* 409.1876 $[M + Na]^+$(calcd for $C_{19}H_{30}O_8Na$ 409.1838). The ^1H and ^{13}C-NMR spectra were almost identical to those of **4**, but with differences in their chemical shifts observed at C-9 due to the change from an oxycarbon to ketone signal. Based on the spectral characteristics and comparison with the prior observed NMR data in the literature,[17] the structure of **6** was deduced as 5,6-epoxy-β-ionone-3-*O*-β-D-glucopyranoside or icariside B2 (Fig. 4).

Three known megastigmane compounds, each containing an epoxy ring, were identified as crotalionoside C (compound **7**),[18] officinoside B (compound **8**),[19] and 5,8-epoxymegastigmane-6-en-3-on 9-*O*-β-D glucopyranoside (compound **9**)[20] by comparison of their spectroscopic data (HR-MS and NMR) with those reported in the literature for the aforementioned compounds (Fig. 4).

Effects of some potential compounds on the production of IL-1β and IL-10 from RAW 264.7 cells treated with LPS

The cytotoxic activity of the compounds boehmegaside A (**1**), (6*S*,9*R*)-roseoside (**2**), akequintoside D (**3**), icariside B2 (**6**) and hydroxytyrosol 4-β-D-glucoside (reported in a previous publication[9]) extracted from an *n*-BuOH fraction was examined against RAW 264.7 cells. The results showed that more than 96% of cells survived when adding these compounds at a concentration of 10 μg mL^{-1}. These compounds were also evaluated for their *in vitro* immunomodulatory activity for inhibiting IL-1β production and stimulating IL-10 production caused by LPS (5 ng mL^{-1}) in RAW 264.7 cells.

Among the 5 tested compounds (10 μg mL^{-1}), 3 megastigmane compounds, namely akequintoside D (**3**), (6*S*,9*R*)-roseoside (**2**), and icariside B2 (**6**), significantly inhibited LPS-induced IL-1β production, with IL-1β concentrations of 72.09, 71.36, and 63.47 pg mL^{-1} compared to the positive control group treated with 5 ng mL^{-1} LPS (465.84 pg mL^{-1}). Additionally, the megastigmane compounds **3** and **6** demonstrated significant stimulation of IL-10 production, with IL-10 concentrations of 260.45 and 267.49 pg mL^{-1}, respectively, compared to the positive control group treated with 5 ng mL^{-1} LPS (105.42 pg mL^{-1}). These results highlight the potential of the isolated compounds, especially the remaining megastigmane compounds, which are considered promising candidates for further exploration for developing immunomodulatory agents.

Molecular docking results

The pro-inflammatory cytokine IL-1β and anti-inflammatory cytokine IL-10 play crucial roles in regulating inflammation as a dynamic process. IL-1β acts on monocytes and macrophages and initiates a series of intracellular signaling events that enhance the immune function.[21] However, the overexpression of IL-1β can be detrimental to the human body.[22] Meanwhile, interleukin 10 is central to limiting the host immune response to pathogens, thereby preventing tissue damage and maintaining normal homeostasis.[23]

Lipopolysaccharide (LPS) is a significant component of the outer membrane of Gram-negative bacteria and stimulates macrophages to produce inflammatory factors and nitric oxide (NO), initiating an inflammatory response.[24] TLR4, the primary

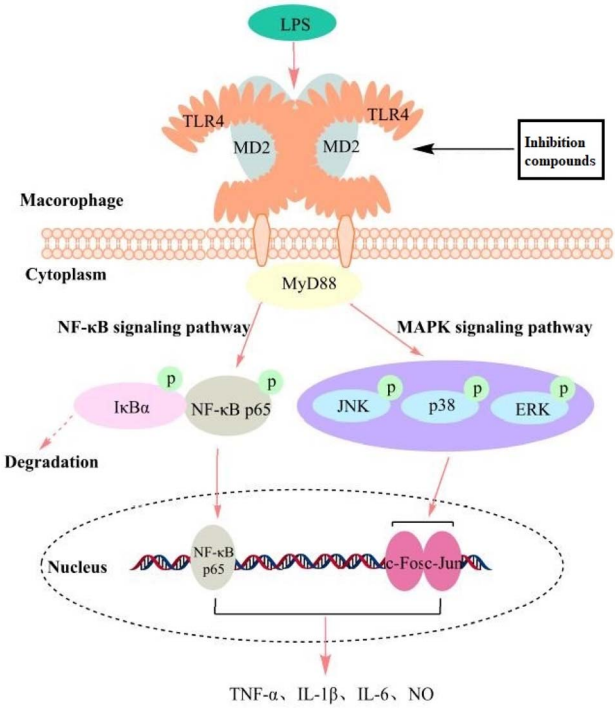

Fig. 5 Mechanism of action of the inhibiting compounds on TLR4, and the diagram of its anti-inflammatory pathway.[28]

LPS receptor on the surface of monocytes, macrophages, and dendritic cells, facilitates innate immunity.[25] It mediates the phagocytic inflammatory response to various microorganisms by activating the NF-κB signaling pathway.[26] The recognition of LPS requires the formation of the TLR4-MD-2 complex, which then binds to LPS to mediate signal transduction and stimulate macrophages to produce an inflammatory response.[27] Therefore, we speculated that the studied compounds could bind to TLR4-MD-2 instead of LPS, thereby blocking the TLR4-MD-2-mediated NF-κB/MAPK signaling pathway and exerting their immunomodulatory effects (Fig. 5).

Numerous compounds have been reported to interact with TLR4-MD-2, exerting either pro-inflammatory or anti-inflammatory effects.[29,30] Thus, molecular docking simulation was performed to clarify the interaction between the studied compounds and TLR4-MD-2. AutoDock4 is among the most popular docking software, with over 6000 citations since 2010.[31–33] It is a valuable tool for rapidly predicting the binding affinity of ligands to specific proteins or enzyme targets. Here, AutoDock4 was utilized for searching for the potential mechanisms of the bioactive compounds. The docking scores are shown in Table 5.

According to the ranking criteria of AutoDock4, a more negative docking energy suggests a higher binding affinity of a compound towards the targeted receptor.[34] The results obtained in the docking study indicated that akequintoside D (**3**), (6*S*,9*R*)-roseoside (**2**), and icariside B2 (**6**) could be assumed as "HITs" based on their docking scores. Considering the compounds suggested to be bioactive in the experiments, the obtained results showed a high correlation. A stereoview of the binding mode of the potential ligands is depicted in Fig. 6.

The active site of TLR4-MD-2 is a pocket mainly composed of TLR4 domain residues and MD-2 domain residues, which have been reported to include the following essential residues: Lys89, Arg90, Val93, Tyr102, Lys125, Lys360 and Arg337.[35] It was observed that the potential compounds did not bind to the hydrophobic pocket in MD-2, which is where LPS bridges TLR4 and MD-2 to initiate signal transduction. Instead, they bound to a cleft primarily formed by TLR4. Fig. 6A reveals that residues Arg337, Gln339, Met358, Lys360, and Arg380 from TLR4, along with His96 from MD-2, created a smooth surface. The planar structures of akequintoside D (**3**), (6*S*,9*R*)-roseoside (**2**) and andicariside B2 (**6**) fit this shape perfectly and adhered closely to the surface.

Of all the docked results, compound **3** exhibited the highest binding affinity (−11.87 kcal mol^{-1}). Analysis of the binding orientation of **3** showed that Val93 and Leu94 were the key residues that participated in hydrophobic interactions. The interaction was further stabilized through H-bonds with Tyr102 and Arg337. In the docking pose of **2**, the hydrophobic pockets formed with this ligand involved residue Val93. The interaction was further strengthened through three conventional hydrogen bonds with Arg337 and Gln339. An array of H-bond interactions was observed to be contributed by Glu92, Val93 and Arg337 for binding with compound **6**. Also, the hydrophobic bond was constituted from the interaction with Lys91.

Megastigmane belongs to the family of terpene compounds with a 13-carbon aglycon framework, including a hydroxyl group and chiral carbon positions mainly at C-6 and C-9. In addition, oxidation reactions at the double bonds or ring closures and glycosylation create structural diversity in the megastigmane group. A review publication in 2017 showed that there were about 230 megastigmane compounds that had been isolated and identified in nature from plant sources, such as Vitaceae, Fabaceae, Apocynaceae, and Berberidaceae.[36] According to the reference article, the publications related to megastigmane compounds to date have been mainly related to their

Table 5 Molecular docking simulation of the compounds with the following parameters: docking score, H-bonds, and interacting residues

Compounds	Docking score (kcal mol^{-1})	No. of H-bonds	Interacting residues
Akequintoside D (compound **3**)	−11.87	3	Val93, Leu94, Tyr102, Arg337
(6*S*,9*R*)-roseoside (compound **2**)	−10.40	3	Val93, Arg337, Gln339
Icariside B2 (compound **6**)	−10.75	3	Lys91, Glu92, Val93, Arg337
Boehmegaside A (compound **1**)	−7.39	2	Val93, His96, Met358, Asn359, Gly361, Asn381
Hydroxytyrosol 4-β-D-glucoside	−7.90	2	Val93, Arg337, Met358, Gly361, Arg380

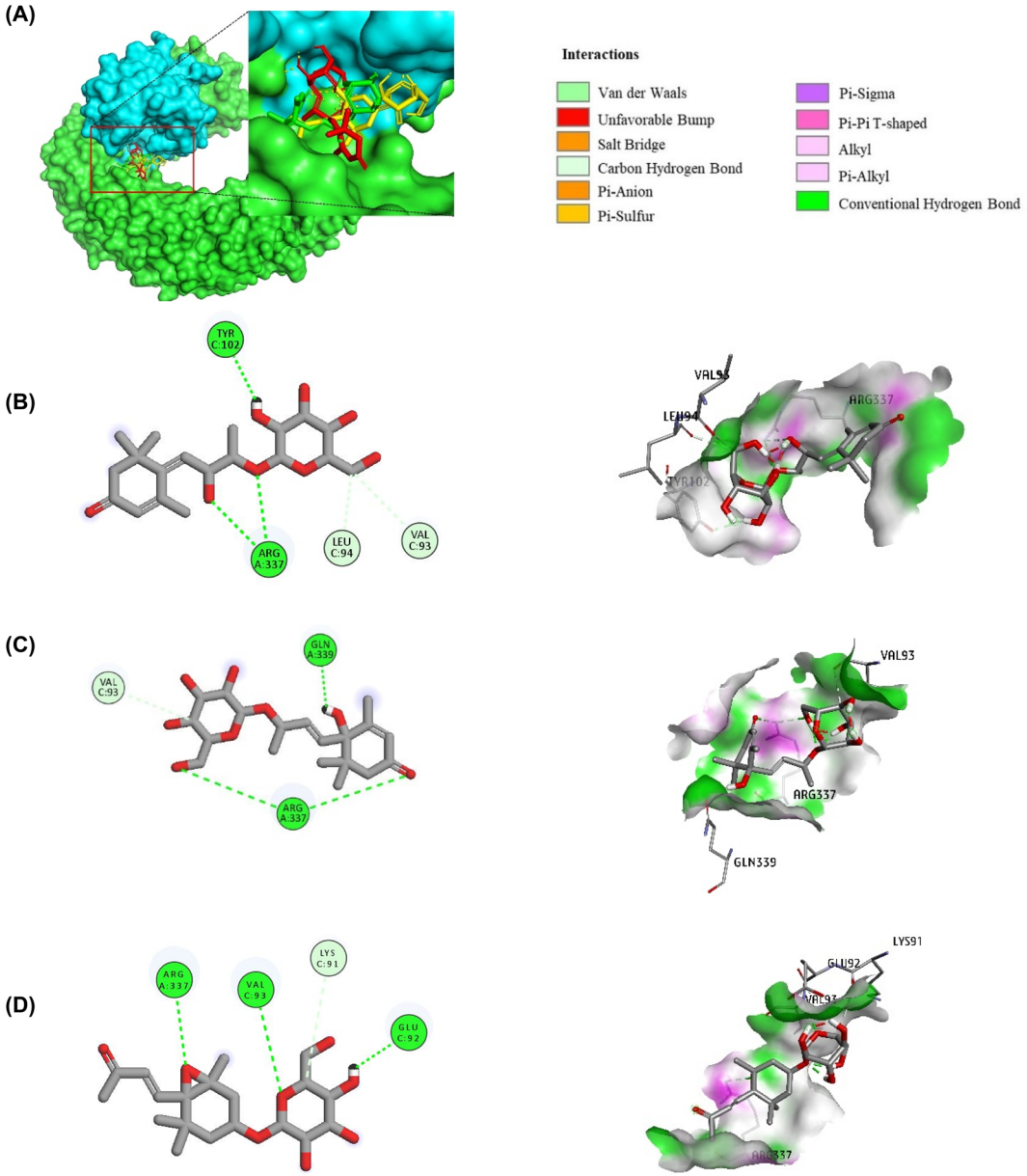

Fig. 6 Binding conformation of the studied compounds revealed by molecular docking simulations. (A) HITs compounds bind to a smooth region in TLR4, adjacent to its contact interface with MD-2: **3**-red, **2**-green, and **6**-yellow. (B) Docking pose of **3**. (C) Docking pose of **2**. (D) Docking pose of **6**.

chemical structures, and rarely associated with their biological effects. This study is the first to report the isolation of megastigman terpenes, specifically a new megastigmane, and eight megastigmane compounds in the genus *Boehmeria*. For the new megastigmane (6*S*,9*R*)-3-oxo-α-ionol-β-D-glucopyranoside, named as boehmegaside A, three isomers of this structural framework have been reported previously as isomers (6*R*,9*R*), (6*R*,9*S*), and (6*S*,9*S*) of 3-oxo-α-ionol-β-D-glucopyranoside.[10,37] Also, some epoxy ring structures were isolated, including alangionoside E, staphylionoside H, officinoside B, and akequintoside D, which are considered rare structures. To the best of our knowledge, alangionoside E was only published in *Alangium premnifolium* (1995)[15] and officinoside B was only published in Egyptian Calendula officinalis (2001),[19] with no biological testing reports yet. This is the second time staphylionoside H has been published in nature.

Besides, previous publications showed that the isolated megastigmane compound akequintoside D was also only published in *Akebia quinata* species (2015), showing a moderate IL-6 production inhibitory activity on TNF-α-stimulated MG-63 cells (40% inhibition of the IL-6 concentration) compared to the positive control group TNF-α 10 ng mL^{-1} ($p < 0.001$).[38] Meanwhile, (6*S*,9*R*)-roseoside was shown to enhance insulin release from the INS-1 cell line in *in vitro* testing.[39] Studies have also synthesized isomers of roseoside[13] and demonstrated that 4 stereoisomers inhibited leukotriene release from cultured mast

cells derived from mouse bone marrow.[40] Another publication showed that (6*S*,9*R*)-roseoside had anti-inflammatory effects on a model for inhibiting NO release on the RAW 264.7 cell line stimulated with LPS, with IC_{50} = 7.31 μM (compared to the control hydrocortisone with IC_{50} = 64.34 μM). Icariside B2 has shown anti-inflammatory effects in *in vitro* tests (on a model using BV2 glial cells stimulated with LPS) and *in vivo* (at a dose of 50 mg kg^{-1}, it showed anti-edema effects in mice in a model of acute inflammation in rat paws with carrageenan) by various proven mechanisms, such as inhibiting the generation of NO and prostaglandin E2 by reducing the expression of inducible NO synthase and cyclooxygenase 2, reducing the expression of the cytokines that cause inflammation (TNF-α, IL-6, and IL-1β) and also hinder phosphorylation of the inhibitory protein κBα, and inhibiting COX-2 enzyme with an IC_{50} value of 7.80 ± 0.26 μM. From the above review, it is evident that the results of immunomodulatory activity studies in *in vitro* and *in silico* tests of akequintoside D (**3**), (6*S*,9*R*)-roseoside (**2**), and icariside B2 (**6**) were also consistent with the published biological results. These findings demonstrate the potential of *B. nivea* leaf extracts and isolated compounds, particularly megastigmane, which are considered promising structures for further in-depth exploration. Further studies into the mechanism of the immunomodulatory and other biological activities of *B. nivea* are warranted.

Experimental

Plant materials

The leaves of *B. nivea* were collected in Tuyen Quang in Vinh Loc town, Chiem Hoa district, Tuyen Quang province, Vietnam in June 2022. The plant material was identified and a voucher specimen was deposited at the Center for Medicinal Resources – Institute of Medicinal Plants, Vietnam National Institute Medicinal Plants (BNL-06/2022-TQ). After collection, the samples were dried in the shade at 45–50 °C and coarsely ground into powder (12.5 kg).

Solvents, chemical reagents, and research equipment

Chemical research. The solvents were purchased from RCI Labscan Ltd (Thailand). The solvents for HPLC analysis (ACN, MeOH) were purchased from JTBaker (USA). Compounds were isolated by column chromatography (CC) with silica gel (Merck, particle size 63–200 mm), RP-C18 (Merck, particle size 40–63 mm), Sephadex LH-20 (25–100 μm), and MCI gel (75–150 μm). Thin-layer chromatography (TLC) was performed on precoated Kieselgel 60F254 and RP-18F254S, and spots were detected under a UV lamp or were visualized by spraying with vanillin-sulfuric acid reagent (VS), followed by heating. NMR spectra were recorded on Bruker Avance Digital 500 and 600 MHz NMR spectrometers (Karlsruhe, Germany) at the Institute of Chemistry, Vietnam Academy of Science and Technology and a Bruker Avance 800 MHz instrument (Bruker, Billerica, MA, USA) at Seoul National University, Korea using tetramethylsilane as an internal standard. ESI low-resolution LC-MS data were recorded using an Agilent Technologies 6130 Quadrupole mass spectrometer (Agilent Technologies, Santa Clara, CA, USA). ESI high-resolution LC-MS/MS data were recorded using a Xevo G2-XS QToF system (Waters, USA). The GC-MS analysis was performed using a Shimadzu GC-MS-QP2010 Plus (Kyoto, Japan), equipped with an Equity®-5 (Supelco) capillary column (30 m × 0.25 mm i.d.).

Bioactivity reagents. The key reagents were: RAW264.7 cells (ATCC, Rockville, MD), FBS bovine serum (Gibco, USA), Dulbecco's modified eagle medium-DMEM (Gibco, USA), penicillin/streptomycin (Biochrom, UK), Goldbio thiazolyl blue tetrazolium bromide – MTT (Sigma), interleukin IL-1β quantification KIT (IL-1β mouse ELISA Kit), and interleukin 10 (IL-10 mouse ELISA Kit) (R&D Systems, USA), and the inflammatory substance LPS (Sigma, USA).

Investigation of the immunomodulatory activity of fractions extracted from BNL and compounds on LPS-induced IL-1β and IL-10 production in RAW 264.7 macrophages

Sample preparation. *B. nivea* leaves powder (100 g) was extracted by an ultrasonic extractor with 500 mL of 70% EtOH at 45 °C for 90 min (300 mL × 3 times). All the extracts were combined and evaporated *in vacuo* to obtain a 70% EtOH extract, and then separated by their liquid–liquid distribution with different solvents to yield *n*-hexane, EtOAc, and *n*-butanol extracts. The extract samples were lyophilized to remove the organic solvents and were then stored in colored vials at 0–4 °C for later use.

Experiments. RAW264.7 macrophage cells were cultured at 37 °C and in 5% CO_2 in DMEM medium containing 10% FCS, 1% penicillin antibiotics (100 IU mL^{-1}), and streptomycin (100 μg mL^{-1}). Then, they were separated, washed, and reconstituted in a new medium, then transferred to 96-well plates at a density of 10^4 cells per well/100 mL overnight with 10% FCS. After 12 h of incubation at 37 °C with 5% CO_2, the cells were stimulated by 5 ng mL^{-1} LPS in the presence or absence of the extracts or isolated compounds (concentrations of the test samples were selected from the MTT toxicity test, by determining the maximum concentration that did not show cytotoxicity for the following tests) and incubated for 24 h. The cultured cell extracts were collected and their IL-1β and IL-10 content measured. This medium was quantified with the ELISA immunochemical technique and the protocol was performed according to the manufacturer's instructions.[41,42] Specifically:

Sample: The fraction extracts and the isolated compounds were dissolved in DMSO (20 and 10 μg mL^{-1}) by vortexing at 300–500 rpm.

Positive control group: Cells were incubated with the inflammatory inducer LPS 5 ng mL^{-1} for 24 h.

Control sample: Cells were incubated with 1% DMSO in the medium.

Statistical analysis. All the experiments were performed 5 times, and the results are represented as the mean ± standard error of the mean (SEM). Statistical significance was determined using the analysis of variance (ANOVA), followed by a Dunnett's test for pairwise comparisons as analyzed with GraphPad Prism

9.5.0 software. Statistical significance was determined as $p < 0.05$.

Extraction and isolation. The air-dried material powder (12.0 kg) was refluxed with 70% EtOH (ratio 1 : 10, 3 times). The extract was filtered, and the solvent was removed by evaporation under low pressure to obtain a 70% EtOH extract (BNL, 1.5 kg). Then, water was added to this crude extract and successively partitioned into *n*-hexane, $CHCl_3$, EtOAc, and *n*-butanol solvents. Finally, five fractions were extracted from BNL: *n*-hexane extract (250 g), chloroform extract (125.42 g), ethyl acetate extract (18.23 g), *n*-butanol extract (92.57 g) and water extract (1013.78 g).

The *n*-butanol extract (70 g) was subjected to column chromatography (CC) with silica gel and eluted with a gradient mixture of $CHCl_3$–MeOH–H_2O solvent (9 : 1 : 1–6 : 4 : 1, v/v) to obtain 19 fractions (Bu1–19). Two fractions, Bu9 (2.3 g) and Bu10 (4.5 g), were CC separated with a saturated EtOAc–MeOH solvent system (95 : 5–85 : 15, v/v) to obtain 10 fractions (Bu9.1–9.10) and 15 fractions (Bu10.1–10.15), respectively. Fraction Bu9.6 (445 mg) was separated by silica gel CC with a mixture of $CHCl_3$–MeOH–$(Me)_2CO$–H_2O solvent (7 : 3 : 1 : 1, v/v) to obtain compound **3** (60.9 mg). Fraction Bu10.7 (938 mg) was separated by Sephadex LH-20 with 100% MeOH to obtain 6 fractions (Bu10.7.1–10.7.6). Compounds **2** (78.8 mg), **4** (69.0 mg), **5** (9.3 mg), and **7** (9.4 mg) were purified from fraction Bu10.7.2 (690 mg) using silica gel RP-C_{18} CC eluted with H_2O–MeOH (4 : 1–3 : 2, v/v), respectively. Fraction Bu10.10 (189 mg) was isolated by silica gel RP-C_{18} CC eluted with a gradient mixture of H_2O–MeOH (3 : 1–3 : 2, v/v) to obtain **9** (3.6 mg) and **8** (3.8 mg). Fraction Bu14 (2.9 g) was applied to Sephadex LH-20 with 100% MeOH to obtain 6 fractions (Bu14.1–14.6). Fraction Bu14.2 (1.58 g) was isolated by silica gel CC with a mixture of EtOAc–MeOH–H_2O solvent (17 : 3 : 4, v/v) to obtain 14 fractions (Bu14.2.1–14.2.14). Fraction Bu14.2.6 (210 mg) was separated by silica gel RP-C_{18} CC eluted with H_2O–MeOH (7 : 3–3 : 2, v/v) to obtain compound **6** (17.2 mg) and compound **1** (8.6 mg).

Determination of the monosaccharide composition of compound 1. Alditol per-acetate derivatives were prepared using the method reported by Ho DV,[43] with slight modifications to the procedure described by Pettolino *et al.*[44]

Computational study for determination of the absolute configurations of compound 1

Conformational searches and geometrical optimization. Compounds (**1a–1d**) were subjected to conformational searches using the molecular mechanics (MMFF) set in Spartan 14. Conformers with a Boltzmann distribution >1% were then DFT optimized by Gaussian 09 (ref. 45) at the B3LYP/6-31G(d) level in the gas phase. Harmonic vibrational frequencies were assessed at the same level to ensure that no imaginary value was present, confirming the stability of the selected conformers. The Gibbs free energy from the frequency calculations was used to calculate the Boltzmann distribution of the conformers.

Calculation of the NMR chemical shifts and DP4+ probabilities. The optimized conformers were subjected to NMR calculations using Gaussian 09 software. The Boltzmann averaged shielding tensors were adjusted to chemical shifts using tetramethylsilane as the reference standard, calculated under the same level of theory and basic set. All the unscaled chemical shifts were used for the DP4+ probability calculation based on the method reported by Sarotti *et al.*[46]

Theoretical calculation of the ECD spectrum. The calculations for the ECD spectra were performed using time-dependent density-functional theory (TDDFT) at the B3LYP/6-31G(d,p) level of theory using the PCM solvent model in MeOH. The calculation was performed for each conformer, and an averaged spectrum was generated based on the Boltzmann population using Specdis v1.71. The half-band was taken at $\zeta = 0.30$ eV and the UV correction was +5 nm.

Molecular docking studies

Since the experiments in this research were conducted on RAW264.7 cells, the crystal structures of the mouse TLR4 and mouse MD-2 complex were chosen for the docking simulations with the compounds boehmegaside A (**1**), (6*S*,9*R*)-roseoside (**2**), akequintoside D (**3**), icariside B2 (**6**) and hydroxytyrosol 4-β-D-glucoside (reported in a previous article[9]). The three-dimensional structure of the TL4/MD-2 complex was downloaded from the RCSB Protein Data Bank with PDB ID: 2Z64.[35] It has been stated that a resolution between 1.5 and 3.0 Å is regarded as good quality for docking studies.[47,48] The primary basis for identifying the putative binding region was the interaction with model 2Z64, a monomeric LPS-free TLR4-MD-2 structure prepared for ligand docking. Subsequently, the active conformation (PDB ID: 3VQ2), a dimeric TLR4/MD-2 complex with LPS, was used to confirm the results. To prepare a free receptor, water molecules were removed from the protein. The protein was then readied for the docking simulations by assigning partial charges, solvation parameters, and hydrogens to the receptor molecule. A grid box was constructed to encompass all the possible binding sites, using validated ligands as references. AutoDock 4.2 was employed for the molecular docking simulations, utilizing the Lamarckian Genetic Algorithm (LGA). The docking conformation with the lowest binding free energy, selected from the most favored cluster, was chosen for further analysis. The results from the AutoDock modeling studies were analyzed using PyMOL and Discovery Studio Visualizer 2010.

Conclusions

This study used bioassay-guided fractionation and purification to isolate the immunomodulatory compounds of extracts from *B. nivea* leaves. From the potential fraction in *n*-BuOH, 9 compounds belonging to the megastigmane family were isolated and identified, marking this the inaugural report of megastigmane compounds in *Boehmeria* genus. Among them, a new megastigmane glycoside was identified, namely boehmegaside A (**1**), and 8 known compounds, namely (6*S*,9*R*)-roseoside (**2**), akequintoside D (**3**), alangionoside E (**4**), staphylionoside H (**5**), icariside B2 (**6**), crotalionoside C (**7**),

officinoside B (**8**), and 5,8-epoxymegastigmane-6-en-3-on-9-*O*-β-D-glucopyranoside (**9**). *In vitro* immunomodulatory activity testing was applied to investigate the immunomodulatory effects by evaluating the production of IL-1β and IL-10 from RAW 264.7 cells treated with LPS. The megastigmane compounds **3**, **2**, and **6** (10 μg mL^{-1}), significantly inhibited LPS-induced IL-1β production, with IL-1β concentrations of 72.09, 71.36, and 63.47 pg mL^{-1} compared to the positive control group treated with 5 ng mL^{-1} LPS (465.84 pg mL^{-1}). Additionally, the megastigmane compounds **3** and **6** (10 μg mL^{-1}) demonstrated a significant stimulation of IL-10 production, with IL-10 concentrations of 260.45 and 267.49 pg mL^{-1}, respectively, compared to the positive control group treated with 5 ng mL^{-1} LPS (105.42 pg mL^{-1}). Moreover, an *in silico* study showed that the planar structures of **3**, **2**, and **6** were critical in their ability to directly suppress TLR4 signaling, as demonstrated by the molecular docking simulations. These three powerful substances did not occupy the binding site in MD-2, in contrast to the interaction between LPS and TLR4. Instead, they attached to a nearby smooth area in TLR4. This probably interfered with TLR4 and MD-2's ability to build their primary contact interface and recognize LPS. These results indicate that TLR4 plays a significant role in inflammation and immunity, which means that these chemicals may be useful for treating various inflammatory illnesses linked to immunological problems.

Data availability

Data supporting this study are included within the article and its ESI.†

Author contributions

Thi Thu Thao Nguyen, Thi Ha Do, and Thi Hong Van Le designed the study; Thi Thu Thao Nguyen performed the isolation and structural elucidation of compounds; Thi Hien Tran, Thi Ha Do and Quoc Ky Truong conducted the analysis of bioactivity; Viet Duc Ho performed computational study to determine the absolute configurations; Vy Anh Tran and Minh Quan Pham carried out molecular docking and molecular dynamics simulation; Thi Hong Van Le, Thi Thu Thao Nguyen, and Vy Anh Tran analyzed, drafted, and revised the manuscript. All the authors read and approved the final manuscript.

Conflicts of interest

There are no conflicts to declare.

Acknowledgements

This study belonged to the research "Study on anti-cancer and immunomodulatory activities of some Vietnamese medicinal plants", grant/award number: NĐT.85.KR/20, contract no. 09/2020/HĐ-NĐT signed 09/9/2020-MOST. We would also like to extend our thanks to the Institute of Medicinal Materials-Ministry of Health for funding this research. Special thanks to Professor Jeong Hill Park (Seoul National University) for his support with NMR analysis and to Mr Mai Hieu for his assistance with $DP4^+$ and ECD recording and analysis.

References

1 L. E. Miller, in *Manual of Laboratory Immunology*, ed. H. R. Ludke, J. E. Peacock and R. Tomar, Lea and Febiger, London, 2nd edn, 1991, pp. 1–57.
2 S. Sisodia, *EJBPS*, 2018, **5**, 163–174.
3 R. N. Apte, S. Dotan, M. Elkabets, M. R. White, E. Reich, Y. Carmi, X. Song, T. Dvozkin, Y. Krelin and E. Voronov, *Cancer Metastasis Rev.*, 2006, **25**, 387–408.
4 R. Sabat, G. Grütz, K. Warszawska, S. Kirsch, E. Witte, K. Wolk and J. Geginat, *Cytokine Growth Factor Rev.*, 2010, **21**, 331–344.
5 X. T. Wang, K. Wong, W. J. Ouyang and S. Rutz, *Cold Spring Harbor Perspect. Biol.*, 2019, **11**, a028548.
6 Q.-M. Xu, Y.-L. Liu, X.-R. Li, X. Li and S.-L. Yang, *Nat. Prod. Res.*, 2011, **25**, 640–647.
7 A. Muhammad Ikhlas, I. Muhamad and F. Irda, *Pharmacogn. J.*, 2021, **13**, 1533–1541.
8 H. Assaf, A. Nafady, A. Allam, A. Hamed and M. Kamel, *J. Adv. Biomedical Pharm. Sci.*, 2020, **3**, 150–176.
9 T. T. T. Nguyen, T. H. Do, D. N. Tran, Q. K. Truong and T. H. V. Le, *J. Med. Mater.*, 2024, **29**, 144–149.
10 A. Pabst, D. Barron, E. Sémon and P. Schreier, *Phytochemistry*, 1992, **31**, 1649–1652.
11 H. Otsuka, M. Yao, K. Kamada and Y. Takeda, *Chem. Pharm. Bull.*, 1995, **43**, 754–759.
12 Y. Zhou, B.-M. Feng, L.-Y. Shi, H.-G. Wang, L. Tang and Y.-Q. Wang, *Nat. Prod. Res.*, 2011, **25**, 1219–1223.
13 Y. Yamano and M. Ito, *Chem. Pharm. Bull.*, 2005, **53**, 541–546.
14 H.-G. Jin, A. R. Kim, H. J. Ko and E.-R. Woo, *Arch. Pharmacal Res.*, 2015, **38**, 591–597.
15 H. Otsuka, K. Kamada, M. Yao, K. Yuasa, I. Kida and Y. Takeda, *Phytochemistry*, 1995, **38**, 1431–1435.
16 Y. Takeda, H. Zhang, T. Matsumoto, H. Otsuka, Y. Oosio, G. Honda, M. Tabata, T. Fujita, H. Sun, E. Sezik and E. Yesilada, *Phytochemistry*, 1997, **44**, 117–120.
17 S.-Y. Lee, I.-K. Lee, S.-U. Choi and K.-R. Lee, *Nat. Prod. Sci.*, 2012, **18**, 166–170.
18 J. Shitamoto, K. Matsunami, H. Otsuka, T. Shinzato and Y. Takeda, *Chem. Pharm. Bull.*, 2010, **58**, 1026–1032.
19 T. Marukami, A. Kishi and M. Yoshikawa, *Chem. Pharm. Bull.*, 2001, **49**, 974–978.
20 T. H. Nguyen, N. Kim Tuyen Pham, K. Pudhom, P. E. Hansen and K. P. Nguyen, *Magn. Reson. Chem.*, 2014, **52**, 795–802.
21 M.-H. Pan, K. Maresz, P.-S. Lee, J.-C. Wu, C.-T. Ho, J. Popko, D. S. Mehta, S. J. Stohs and V. Badmaev, *J. Med. Food*, 2016, **19**, 663–669.
22 Y. Yang, R. Xing, S. Liu, Y. Qin, K. Li, H. Yu and P. Li, *Int. J. Biol. Macromol.*, 2018, **108**, 1310–1321.
23 S. S. Iyer and G. Cheng, *Crit. Rev. Immunol.*, 2012, **32**, 23–63.
24 W. A. H. M. Karunarathne, K. T. Lee, Y. H. Choi, C.-Y. Jin and G.-Y. Kim, *Phytomedicine*, 2020, **76**, 153237.
25 B. S. Park and J.-O. Lee, *Exp. Mol. Med.*, 2013, **45**, e66.

26 F. Li, P. Du, W. Yang, D. Huang, S. Nie and M. Xie, *Int. J. Biol. Macromol.*, 2020, **164**, 2134–2140.
27 Y. Sun, Z. Liu, S. Song, B. Zhu, L. Zhao, J. Jiang, N. Liu, J. Wang and X. Chen, *Int. J. Biol. Macromol.*, 2020, **146**, 931–938.
28 L. Li, H. Chen, G. Huang, Y. Lv, L. Yao, Z. Guo, S. Qiu, X. Wang and C. Wei, *Foods*, 2024, **13**, 1356.
29 H. Xu, M. Liu, G. Chen, Y. Wu, L. Xie, X. Han, G. Zhang, Z. Tan, W. Ding, H. Fan, H. Chen, B. Liu and Y. Zhou, *Front. Pharmacol.*, 2022, **13**, 714554.
30 X.-r. Zhang, C.-h. Qi, J.-p. Cheng, G. Liu, L.-j. Huang, Z.-f. Wang, W.-x. Zhou and Y.-x. Zhang, *Int. Immunopharmacol.*, 2014, **19**, 132–141.
31 N. T. Dan, H. D. Quang, V. Van Truong, D. Huu Nghi, N. M. Cuong, T. D. Cuong, T. Q. Toan, L. G. Bach, N. H. T. Anh, N. T. Mai, N. T. Lan, L. Van Chinh and P. M. Quan, *Sci. Rep.*, 2020, **10**, 11429.
32 S. T. Ngo, N. M. Tam, M. Q. Pham and T. H. Nguyen, *J. Chem. Inf. Model.*, 2021, **61**, 2302–2312.
33 N. T. Nguyen, T. H. Nguyen, T. N. H. Pham, N. T. Huy, M. V. Bay, M. Q. Pham, P. C. Nam, V. V. Vu and S. T. Ngo, *J. Chem. Inf. Model.*, 2019, **60**, 204–211.
34 Q. A. Ngo, T. H. N. Thi, M. Q. Pham, D. Delfino and T. T. Do, *Mol. Divers.*, 2020, **25**, 2307–2319.
35 H. M. Kim, B. S. Park, J.-I. Kim, S. E. Kim, J. Lee, S. C. Oh, P. Enkhbayar, N. Matsushima, H. Lee, O. J. Yoo and J.-O. Lee, *Cell*, 2007, **130**, 906–917.
36 S. Ayinampudi, *Chem. Int.*, 2017, **3**, 69–91.
37 E. H. Lee, H. J. Kim, Y. S. Song, C. Jin, K. T. Lee, J. Cho and Y. S. Lee, *Arch. Pharm. Res.*, 2003, **26**, 1018–1023.
38 H.-G. Jin, A. R. Kim, H. J. Ko and E.-R. Woo, *Arch. Pharmacal Res.*, 2015, **38**, 591–597.
39 N. Frankish, F. de Sousa Menezes, C. Mills and H. Sheridan, *Planta Med.*, 2010, **76**, 995–997.
40 A. Yajima, Y. Oono, R. Nakagawa, T. Nukada and G. Yabuta, *Bioorg. Med. Chem.*, 2009, **17**, 189–194.
41 Q. H. Jin, C. Lee, J. W. Lee, E. T. Yeon, D. H. Lee, S. B. Han, J. T. Hong, Y. S. Kim, M. K. Lee and B. Y. Hwang, *J. Nat. Prod.*, 2014, **77**, 1724–1728.
42 Y. J. Jeon, S. H. Han, Y. W. Lee, M. Lee, K. H. Yang and H. M. Kim, *Immunopharmacology*, 2000, **48**, 173–183.
43 D. V. Ho, H. N. T. Hoang, H. Q. Vo, K. V. Nguyen, T. V. Pham, A. T. Le, K. Van Phan, H. M. Nguyen, H. Morita and H. T. Nguyen, *J. Nat. Med.*, 2020, **74**, 591–598.
44 F. A. Pettolino, C. Walsh, G. B. Fincher and A. Bacic, *Nat. Protoc.*, 2012, **7**, 1590–1607.
45 M. Frisch, G. Trucks, H. Schlegel and A. Allam, *Gaussian 09, Revision D. 01*, Gaussian, Inc., Wallingford CT, 2009.
46 N. Grimblat, M. M. Zanardi and A. M. Sarotti, *J. Org. Chem.*, 2015, **80**, 12526–12534.
47 C. Didierjean and F. Tête-Favier, *Acta Crystallogr., Sect. D: Struct. Biol.*, 2016, **72**, 1308–1309.
48 C. Venugopal, C. Demos, K. Jagannatha Rao, M. Pappolla and K. Sambamurti, *CNS Neurol. Disord. :Drug Targets*, 2008, **7**, 278–294.